

Impinging free jets of ideal fluid

By J. HUREAU AND R. WEBER

Laboratoire de Mécanique et d'Énergétique, Ecole Supérieure de l'Énergie et des Matériaux,
Université d'Orléans, Rue Léonard de Vinci, 45072 Orleans Cedex 2, France

(Received 23 May 1997 and in revised form 13 March 1998)

This paper studies the impinging of two ideal fluid jets. The usual two-dimensional model of jet flow uses an ideal, incompressible, weightless fluid to describe these impinging jets, so that the problem becomes one of complex analysis which seems to have an infinite number of analytical solutions, except for direct jet impacts. The new approach presented here is based on the construction of a dividing line between the two jets. It gives an efficient procedure for solving this problem numerically when the jets flow in arbitrary directions and the solution obtained seems to be unique.

1. Introduction

As far back as 1868, Helmholtz and Kirchhoff set up the classical two-dimensional theory of jets. They considered steady irrotational flows of ideal incompressible weightless fluid, bounded by walls and free streamlines. High-speed liquid jets in a stationary gas can be modelled on these assumptions. By the beginning of this century, a great many different kinds of flows could be represented on the basis of complex analysis. The monographs of Birkhoff & Zarantonello (1957), Jacob (1959), Gurevich (1966) and Milne-Thomson (1968) give good surveys of these flows.

The different problems addressed in the theory of jets can be grouped into two main categories. The first comprises problems of plane flows issuing from vessels. The purpose is to define the shape of the free streamlines and the contraction coefficient of the jet for a given nozzle geometry. The main difficulty here stems from the shape of the walls. Solutions were first found by specifying a boundary consisting of a few plate walls. Dias, Elcrat & Trefethen (1987) present an efficient procedure for solving this jet problem numerically, for an arbitrary polygonal nozzle. Later, Dias & Vanden-Broeck (1990) considered a jet flow with gravity.

The second category of problems concerns jets flowing past a wall, the impact of a jet on an obstacle or infinite wall, free jets, and impinging free jets. Except for very simple barrier geometries, these flow problems cannot be solved analytically, as was shown in the monographs mentioned above. King & Bloor (1990) presented a method for determining the free streamline of a jet of ideal fluid flowing past a wall of arbitrary shape. They used the generalized Schwarz–Christoffel transformation combined with a Fourier transform technique to formulate a system of nonlinear integro-differential equations for the tangential angle made by the free surface and the wall. Proceeding similarly Peng & Parker (1997) determined the free surface of a jet impinging on an uneven wall by combining the Hilbert transform with the generalized Schwarz–Christoffel transformation technique. They noted that, when the flow pattern is asymmetrical, the unknown position of the stagnation point makes the free-surface shapes very difficult to compute. Hureau, Brunon & Legallais (1996) proposed a new approach, based on previous studies of Helmholtz flows (see Hureau,

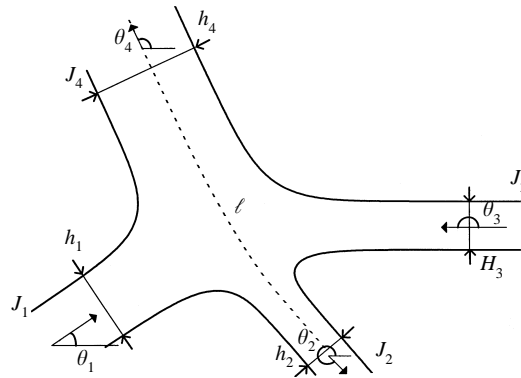


FIGURE 1. General configuration of two impinging free jets.

Mudry & Nieto 1987), using a numerical procedure for the case of a jet impacting and divided by a curved obstacle. The method is efficient and easy enough for us to consider the classical problem of the flow of two impinging free jets.

Consider two impinging jets J_1 and J_3 , of the same speed at infinity, and two outgoing jets J_2 and J_4 (figure 1). The pressure and velocity norms on all the free streamlines are identical. We denote the thickness of the jets at infinity by h_1 , h_2 , h_3 , and h_4 , and the angle between jet directions and the x -axis by θ_1 , θ_2 , θ_3 , and θ_4 , respectively. The problem is determined by the thicknesses h_1 and h_3 , and the angles θ_1 and θ_3 . This problem has been considered by a number of authors, such as Birkhoff & Zarantonello (1957), Gurevich (1966), and Milne-Thomson (1968). It is well known that, if the jets J_1 and J_3 are not parallel to one another and have different thicknesses, the problem appears to be indeterminate because we have only three equations for calculating h_2 , h_4 , θ_2 , and θ_4 . These equations are obtained by applying conservation of mass and the theorem of change of momentum. Various explanations, usually having to do with the stability of the phenomenon, have been proposed for this indeterminateness. Since the purpose of the present study is to model the impact of two physical jets, we have to investigate this question of an infinite number of solutions, because experimental data do not seem to reflect that different flow patterns are possible with just one critical point for two given impinging jets. So what if we determined of this flow pattern by the theorem of change of momentum? We take the example of the impact of a jet on a large plane barrier, and symmetric flow. This configuration is used to solve the impact of two equal jets with incidence (see Milne-Thomson). The theorem is applied to the domain bounded by portions of free streamlines and by cross-cuts joining adjacent free streamlines (figure 2). In order for the velocity to be considered uniform on these cross-cut lines, they must be at a large distance from the impinging area. Figure 3(a) shows the flow of two parallel jets of the same width impinging a large barrier, and 3(b) shows a similar flow when the barrier is not planar. These flow patterns verify the three equations of conservation of mass and change of momentum, but the theorem cannot account for the existence of these barriers inside the domain. We would have the same results even if the impinging jets were shifted, or if a stagnation zone existed (see Gurevich, figure 171 p. 247). So, it appears that the theorem of change of momentum and conservation of mass are not sufficient for solving the impact of two given jets with one critical point, and therefore there is no proof that an infinite number of solutions to this flow pattern exist if a fourth condition is specified.

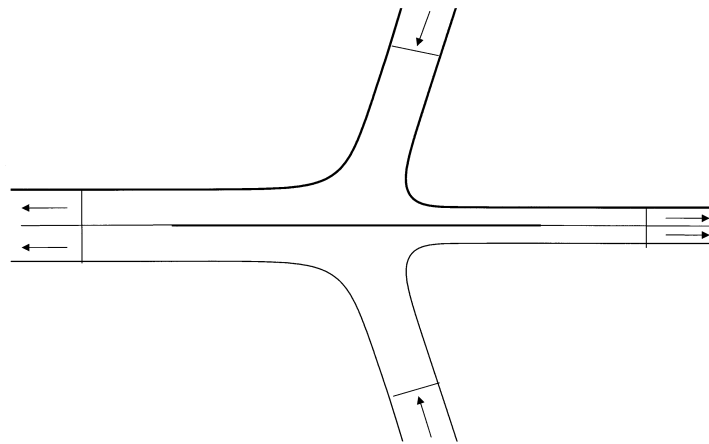


FIGURE 2. Symmetrical jets impinging on a large plate.

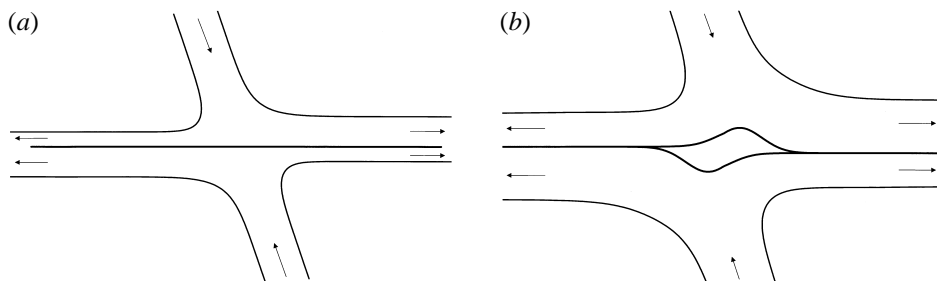


FIGURE 3. Other solutions verifying the theorem of change of momentum.

Gurevich, and then Milne-Thomson, give the equation of the free streamlines in terms of the complex velocity and then of the four unknowns. By applying this equation to a point at infinity of the upper free streamline of jet J_1 , Keller (1990) obtains a new relation giving the distance y_L of the asymptote from the stagnation point. He maintains that if y_L is specified, he has the fourth equation of the problem. He illustrates the use of his equations with the special case of the impact of two equal and oppositely directed jets ($h_1 = h_3$, $\theta_1 = 0$, and $\theta_3 = \pi$), and finds the same results as Birkhoff & Zarantonello and Gurevich. However, no more general case is dealt with, such as the oblique impact of two jets of different thicknesses. Nor is the existence of the solution studied. That is, if the solution is assumed to be unique for two given impinging jets, how can we specify the value of y_L ? Keller's equation does not seem to be the fourth equation, but rather a relation which is obviously verified when the solution is reached. So it seems that there is as yet no solution to oblique impinging jets of different widths. The difficulty in these problems is to determine the position of the stagnation point in the physical plane, as specified by Peng & Parker (1997) for the impact of a jet onto a wall.

Assuming that a solution does exist, we present an efficient numerical method for computing θ_2 , θ_4 , h_2 , h_4 , and the free streamlines by a new approach.

2. Formulation of the problem

After these remarks on the use of the theorem of change of momentum, we have to impose a condition to be sure that the flow pattern is really the one we want. This

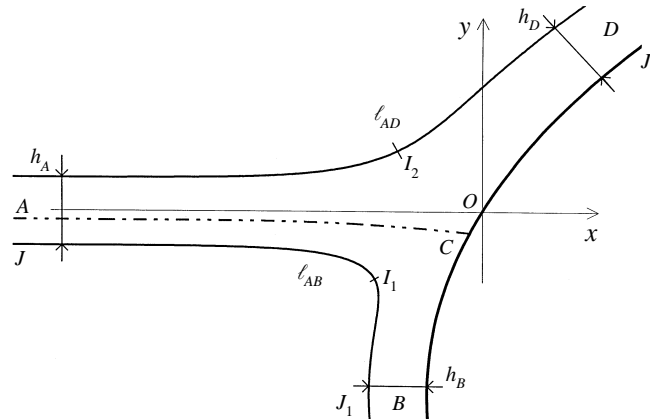


FIGURE 4. Jet impinging on an infinite wall.

condition is that a unique streamline ℓ in equilibrium separates the two impinging jets J_1 and J_3 ; and this is certainly not the case for the infinite solutions given by the theorem of change of momentum and the conservation of mass. To avoid having to verify this condition for each solution, we impose it by constructing ℓ . We likened ℓ to a wall impinged by J_1 , and calculated the velocity distribution along ℓ . Then we determined the shape that ℓ would have if the velocities due to the action of J_3 on this wall were the same as those resulting from the impact of J_1 on ℓ . We then modify the geometry of ℓ , and the procedure is repeated until the shape of ℓ remains unchanged for two iterations.

This led us to review two important previous studies. First, in considering the impact of a jet on an infinite curved wall to obtain the velocity distribution along ℓ , i.e. the direct problem, our method is different from the one developed by King & Bloor (1990) and Peng & Parker (1997). It enables us to consider an inclined jet and a wall with a curvature resembling the one expected for ℓ . Secondly, we formulate a method for designing a wall that corresponds to a prescribed speed distribution, i.e. the inverse problem, which we solve by generalizing an airfoil design method presented by Hureau & Legallais (1996). The formulation used here to construct ℓ works only with the results obtained by solving the impact of a jet on a barrier, and so is not a general solution to the inverse problem. We have to relate these two problems in order to draw the streamline ℓ from the datum of an initial arbitrary shape.

The theorem of change of momentum is not used for solving the problem, but only for checking our results.

3. Jet impinging on an infinite wall

Take a jet J of width h_A and velocity V_∞ , bounded by the free streamlines ℓ_{AB} and ℓ_{AD} , impinging a curved infinite barrier and divided into two branches J_1 and J_2 , as in figure 4. Let C denote the dividing point, A the infinite upstream point, and B and D the infinite downstream points where the widths are h_B and h_D . We choose to define the cartesian x -axis as the centreline of the impinging jet. The origin O of this coordinate system is located at the intersection of the x -axis and the barrier. This is a special case of the impact of a jet on an obstacle (figure 5), presented previously by Hureau *et al.* (1996), because the wetted wall becomes infinite ($B \rightarrow B'$ and $D \rightarrow D'$).

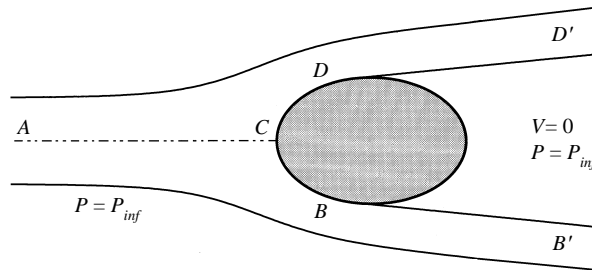


FIGURE 5. Jet impinging on an obstacle.

The physical plane is described by expressing the complex position $z = \int df/w$, where f is the complex potential and w the complex velocity. The boundary conditions are

$$\lim_{z \rightarrow A} w(z) = V_\infty, \tag{3.1}$$

$$\text{Im} \{w(z)dz\} = 0 \quad \text{on the wetted wall } BCD, \tag{3.2}$$

$$|w(z)| = V_\infty \quad \text{on } \ell_{AB} \text{ and } \ell_{AD}. \tag{3.3}$$

3.1. Mathematical formulation

The aim of the problem is to define the flow region in the physical plane by calculating the free streamlines ℓ_{AB} and ℓ_{AD} . This is usually done by conformal mapping of the flow pattern in the f - and w -planes on an auxiliary plane ζ . The flow domain in the f -plane is a strip of width $h_A V_\infty$ (figure 6), but when the wall is curved, the region of variation in the w -plane is unknown. The problem is solved rather by determining the function Ω defined by

$$\Omega = -i \log \frac{V_\infty}{w} = \Theta + iT,$$

where Θ is the direction of the velocity and T is given by $|V| = V_\infty e^T$. T is null on ℓ_{AB} and ℓ_{AD} (3.3), and Θ is assumed to be determined by the shape of the barrier (3.2) on which β is the angle between the tangent at a given point and the x -axis, and s is the arc length starting from O , $s \in]-\infty, +\infty[$. Calculating Ω consists in solving a mixed boundary problem. Using the Levi-Civita method (1907), the flow domain in the z -plane is mapped onto a half-unit disk, in such a way that the free streamlines map onto the diameter. As $\Omega(\zeta)$ tends continuously toward real values on it ($T = 0$) and, according to Schwarz's reflection principle, the Ω -function may be continued analytically across BAD to the lower half-unit disk. The mixed boundary problem then becomes a Dirichlet problem, because $\theta(\sigma) = \Theta(e^{i\sigma})$, or $\tau(\sigma) = T(e^{i\sigma})$, is known everywhere on the circle when we study the direct, or inverse, problem, respectively. Ω is calculated inside the whole disk by the Schwarz-Villat formula. Figure 6 shows the different planes we used to map the flow pattern.

The Schwarz-Christoffel formula is used to map Z onto the f -plane

$$f(Z) = \frac{K}{2} [(1 + \cos \gamma) \log(Z - 1) + (1 - \cos \gamma) \log(Z + 1)] + \text{const.},$$

where the value of K has to be determined and $\zeta = e^{i\gamma}$ corresponds to the point C . By analysing $f(Z)$ in the vicinity of points B and D in the f and the Z -planes, we

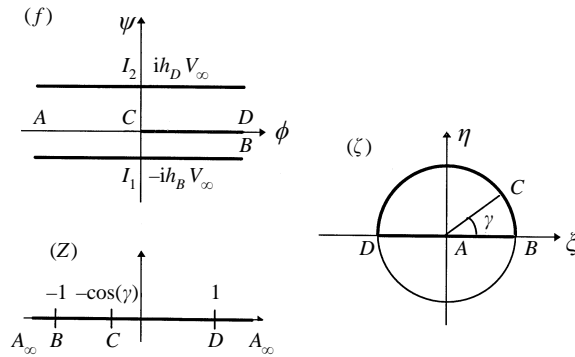


FIGURE 6. Mapping planes.

find the two relations

$$ih_B V_\infty = -i\pi \frac{K}{2} (1 - \cos \gamma),$$

$$ih_D V_\infty = -i\pi \frac{K}{2} (1 + \cos \gamma),$$

and thereby

$$\frac{h_B}{h_D} = \frac{1 - \cos \gamma}{1 + \cos \gamma}.$$

Thus, using the relation $Z = -\frac{1}{2}(\zeta + 1/\zeta)$ to map ζ onto the Z -plane, we have

$$f(\zeta) = -\frac{h_B V_\infty}{\pi} \log \left[1 - \frac{1}{2} \left(\zeta + \frac{1}{\zeta} \right) \right] - \frac{h_D V_\infty}{\pi} \log \left[-1 - \frac{1}{2} \left(\zeta + \frac{1}{\zeta} \right) \right] + \text{const.}$$

Finally

$$df = \frac{V_\infty}{\pi} \left(\frac{h_B}{2 - \zeta - 1/\zeta} - \frac{h_D}{2 + \zeta + 1/\zeta} \right) \left(1 - \frac{1}{\zeta^2} \right) d\zeta. \tag{3.4}$$

Let ϵ be the one-to-one correspondence function between the wetted wall BCD in the ζ -plane and the z -plane

$$\theta(\sigma) = (\beta \circ \epsilon)(\sigma) = \begin{cases} \pi & \text{for } \sigma \in [0, \gamma[\\ 0 & \text{for } \sigma \in]\gamma, \pi]. \end{cases} \tag{3.5}$$

At the stagnation point C , θ has two values, and the null velocity implies that $\tau \rightarrow -\infty$ here, so the Ω -function has a singularity at this point. The usual way of isolating this singularity is to separate Ω into one regular function $\tilde{\Omega}$ and another function Ω_S having the same discontinuity. Moreover, if $\Omega(\zeta)$ becomes infinite as $\zeta \rightarrow e^{i\gamma}$, the same must happen as $\zeta \rightarrow e^{-i\gamma}$, in accordance with the Schwarz reflection principle. Gurevich (1966) proposed a function which satisfies these conditions:

$$\Omega_S(\sigma) = \theta_S(\sigma) + i\tau_S(\sigma) = -\frac{3\pi}{2} + \gamma + i \log \left(\frac{e^{i\sigma} - e^{i\gamma}}{e^{i\sigma} - e^{-i\gamma}} \right),$$

where

$$\theta_S = \begin{cases} -\frac{1}{2}\pi & \text{for } \sigma \in [0, \gamma[\\ +\frac{1}{2}\pi & \text{for } \sigma \in]\gamma, \pi] \end{cases} \quad \text{and} \quad \tau_S = \ln \left| \frac{\sin \frac{1}{2}(\sigma - \gamma)}{\sin \frac{1}{2}(\sigma + \gamma)} \right|.$$

The regular function $\tilde{\Omega} = \tilde{\theta} + i\tilde{\tau}$ must now be found. Here, the treatment of the

two problems (direct and inverse) differs. For the direct problem, the geometry of the barrier is specified and, with (3.5), $\tilde{\theta}$ is known:

$$\tilde{\theta}(\sigma) = \theta(\sigma) - \theta_S(\sigma) = (\beta \circ \epsilon)(\sigma) - \frac{1}{2}\pi. \tag{3.6}$$

On the other hand, in the inverse problem, the prescribed speed distribution yields $\tilde{\tau}$:

$$\tilde{\tau}(\sigma) = \tau(\sigma) - \ln \left| \frac{\sin \frac{1}{2}(\sigma - \gamma)}{\sin \frac{1}{2}(\sigma + \gamma)} \right|. \tag{3.7}$$

3.1.1. Direct problem

In this case, $\tilde{\Omega}$ may be obtained from the Schwarz–Villat formula:

$$\tilde{\tau}(\sigma) = \frac{1}{\pi} \lim_{\zeta \rightarrow e^{i\sigma}} \text{Im} \left\{ \int_0^\pi \frac{1 - \zeta}{1 - 2\zeta \cos \sigma' + \zeta^2} \tilde{\theta}(\sigma') d\sigma' \right\} + \tilde{T}(\zeta = 0), \tag{3.8}$$

for $\tilde{T}(\zeta = 0) = 0$.

From equation (3.1), $\Omega(0) = 0$, and the Schwarz–Villat equation written for Ω at point $\zeta = 0$ yields $\Omega(0) = \int_0^\pi \theta(\sigma') d\sigma'$. Hence

$$\int_0^\pi \tilde{\theta}(\sigma') d\sigma' - \int_0^\gamma \frac{1}{2}\pi d\sigma' + \int_\gamma^\pi \frac{1}{2}\pi d\sigma' = 0,$$

and finally

$$\gamma = \frac{1}{2}\pi + \frac{1}{\pi} \int_0^\pi \tilde{\theta}(\sigma') d\sigma'. \tag{3.9}$$

Then the different terms of the relation

$$dz = \frac{df}{w} = \frac{df}{V_\infty} e^{i[\Omega_S(\sigma) + \tilde{\Omega}(\sigma)]} \tag{3.10}$$

seem to be determined. However equation (3.6) depends on the ϵ -function, which is defined only by the norm of dz (3.10) on the wall, and applying equation (3.4) with $\zeta = e^{i\sigma}$, we finally obtain

$$\epsilon(\sigma) = \int_\gamma^\sigma ds = \frac{2h_A}{\pi} \int_\gamma^\sigma \frac{1}{e^{\tilde{\tau}(\sigma')}} \frac{\sin^2 \frac{1}{2}(\sigma' + \gamma)}{|\sin \sigma'|} d\sigma'. \tag{3.11}$$

In this expression, the stagnation point C has been chosen as reference point because its position in the ζ -plane is determined; but its position in the physical plane, where O is the origin, is unknown. The stagnation streamline ℓ_{AC} for the impinging jet J , computed with respect to the jet axis, gives us the relation

$$\text{Im} \left\{ z_C + \int_{\ell_{AC}} dz \right\} = \frac{h_A}{2} - h_D, \tag{3.12}$$

and then the position of C in the z -plane, i.e. its arc length λ_C on the wall.

3.1.2. Inverse problem

In order to solve the inverse problem, the imaginary part of $\tilde{\Omega}$ is known from the specified speed distribution $e^{\tau(s)}$ (3.7). Another Schwarz–Villat formula should be used to determine the real part $\tilde{\theta}$:

$$\tilde{\theta}(\sigma) = \tilde{\Theta}(\zeta) = \frac{1}{2}\pi \lim_{\zeta \rightarrow e^{i\sigma}} \text{Re} \left\{ \int_0^\pi \frac{\zeta \sin \sigma'}{1 - 2\zeta \cos \sigma' + \zeta^2} \tilde{\tau}(\sigma') d\sigma' \right\} + \tilde{\Theta}(0),$$

where $\tilde{\Theta}(0) = \Theta(0) - \Theta_S(0) = 0 - (\gamma - \frac{3}{2}\pi) + (\gamma - \pi) + (\gamma - \pi)$ with $\Theta(0) = 0$ because the direction of the x -axis has been chosen to coincide with that of the jet. Therefore,

$$\tilde{\Theta}(0) = \gamma - \frac{1}{2}\pi.$$

This yields

$$\tilde{\theta}(\sigma) = \frac{2}{\pi} \lim_{\zeta \rightarrow e^{i\sigma}} \operatorname{Re} \left\{ \int_0^\pi \frac{\zeta \sin \sigma'}{1 - 2\zeta \cos \sigma' + \zeta^2} \tilde{\tau}(\sigma') d\sigma' \right\} + \gamma - \frac{1}{2}\pi. \quad (3.13)$$

As the velocity is zero at the dividing point, it is easy to locate in the prescribed speed distribution (which gives λ_C). We should point out that γ must be obtained immediately from the definition of the function ϵ . But as the arc lengths from the origin become infinite at B and D , the location of γ is not prescribed as it is in airfoil design, where the arc length is finite. The general analysis for asymmetrical barriers is not performed here (this is under consideration) but our present analysis is sufficient for our treatment of impinging jets. So it will be reduced to a symmetrical velocity distribution ($\gamma = \frac{1}{2}\pi$) or to cases where γ could be specified in some another way.

The equation (3.11) that determines the function ϵ is still valid because the expression for df (3.4) is the same. Since the value of λ_C is already known, the additional equation (3.12) is of no use in solving the problem. But with no loss of generality, the initial speed distribution can be given with the origin located at the stagnation point rather than at the point O defined above. The treatment will be exactly the same, but in the end, we will have to draw the stagnation streamline to define the location of the impinging jet. The aim is to draw the wall. This is done by using $dz = dse^{i\theta(\sigma)}$:

$$z(\sigma) = z_C + \frac{2h_A}{\pi} \int_\gamma^\sigma \frac{1}{e^{\tilde{\tau}(\sigma') - i\theta(\sigma')}} \frac{\sin^2 \frac{1}{2}(\sigma' + \gamma)}{|\sin \sigma'|} d\sigma' \quad (3.14)$$

where z_C is found by stating that if $e^{i\sigma_0}$ is the location of point O in the ζ -plane, $z(\sigma_0) = 0$.

3.2. Numerical procedure

The unknowns in the direct problem are the functions $\epsilon, \sigma \rightarrow \tilde{\theta}, \tilde{\tau}$, the angle γ , and the location λ_C of the point C on the wall. Relations (3.11), (3.6), (3.8), (3.9) and (3.12) supply a functional system of five equations written as

$$\epsilon = f_1(\tilde{\tau}, \gamma, \lambda_C), \quad \tilde{\theta} = f_2(\epsilon), \quad \tilde{\tau} = f_3(\tilde{\theta}, \epsilon), \quad \gamma = f_4(\tilde{\theta}, \epsilon), \quad \lambda_C = f_5(\tilde{\tau}, \gamma, \epsilon).$$

This system is solved by building a series $(\epsilon_n, \tilde{\theta}_n, \tilde{\tau}_n, \gamma_n, \lambda_{Cn})$ from any initial correspondence function ϵ_1 , using the following recursive algorithm:

$$\begin{aligned} \epsilon_n &= (1 - r_1)f_1(\tilde{\tau}_{n-1}, \gamma_{n-1}, \lambda_{Cn-1}) + r_1\epsilon_{n-1}, \\ \tilde{\theta}_n &= (1 - r_2)f_2(\epsilon_n) + r_2\tilde{\theta}_{n-1}, \\ \tilde{\tau}_n &= (1 - r_3)f_3(\tilde{\theta}_n, \epsilon_n) + r_3\tilde{\tau}_{n-1}, \\ \gamma_n &= (1 - r_4)f_4(\tilde{\theta}_n, \epsilon_n) + r_4\gamma_{n-1}, \\ \lambda_{Cn} &= (1 - r_5)f_5(\tilde{\tau}_n, \gamma_n, \epsilon_n) + r_5\lambda_{Cn-1}. \end{aligned}$$

The weighting factor r_1 varies from 0.5 to 0.9 for barriers with large curvature, and we choose to leave the others null. The convergence of the problem is verified by a test on the relative error associated with ϵ .

For the inverse problem, the unknowns are the functions $\sigma \rightarrow \tilde{\tau}, \tilde{\theta}, \epsilon$, and the angle β (or θ). In accordance with the preceding remark about the determination of γ , we

assume that the value of γ is specified. The functional system is then reduced to the equations (3.7) and (3.11):

$$\begin{aligned}\tilde{\tau} &= f_1(\epsilon), \\ \epsilon &= f_2(\tilde{\tau}),\end{aligned}$$

and, from an initial function ϵ_0 , we solve by using the following recursive scheme:

$$\begin{aligned}\tilde{\tau}_n &= (1 - r_1)f_1(\epsilon_{n-1}) + r_1\tilde{\tau}_{n-1}, \\ \epsilon_n &= (1 - r_2)f_2(\tilde{\tau}_n) + r_2\epsilon_{n-1}.\end{aligned}$$

Usually, the weighting factor r_2 belongs to [0.5,0.9] while r_1 is set at zero. We stop the process when it converges, as determined by a test on the relative error associated with ϵ .

As expressed previously (3.14), the design of the barrier is defined by relations (3.6) and (3.13).

To solve the flow pattern in these two cases (direct and inverse problem), we still have to draw the free streamlines ℓ_{AB} and ℓ_{AD} . To do this, the reference points I_1 and I_2 , defined in the f -plane are used. Their affixes in the ζ -plane are ζ_{I_1} and ζ_{I_2} , respectively. Their position in the physical plane is obtained by integrating $\int_{\zeta=e^v}^{\zeta_{I_{1,2}}} dz$, where dz is given by (3.10). Then $\int_{\zeta_{I_1}}^{\zeta \rightarrow 1} dz$ and $\int_{\zeta_{I_1}}^{\zeta \rightarrow 0} dz$ are used to draw ℓ_{AB} , and $\int_{\zeta_{I_2}}^{\zeta \rightarrow -1} dz$ and $\int_{\zeta_{I_2}}^{\zeta \rightarrow 0} dz$ to draw ℓ_{AD} .

3.3. Computed results

We will now test the ability of our method by comparing our computed results with analytical or published data.

3.3.1. Direct problem

Convergence is reached after 15 to 20 iterations, requiring a few minutes of calculation on a PC Pentium 120 MHz computer.

Analytical results: The classical analytical solutions are as follows

(i) Impact of a jet on an inclined plate wall. To solve this problem, Milne-Thomson (1968) considers the oblique impact of two equal jets. The bisector of the angles of the two impinging jets is indeed the dividing streamline of the flow, and can be regarded as a rigid barrier. This case of impinging jets is solved analytically.

(ii) Impact of a jet on an infinite wedge. This problem can be reduced to the upper half of the flow, for reasons of flow symmetry. Here, the region of variation in the w -plane is known, but it is usually better to consider the Q -plane, with Q being the Kirchhoff function $Q = \log(V_\infty/w)$. It is then possible to map the Q -plane and f -plane conformally onto the upper half-plane ζ using the Schwarz–Christoffel formula. The free streamline is then calculated by integrating the relation $dz = df e^{Q(\zeta)/V_\infty}$.

In these two cases, the analytical and the computed results are identical.

Published results.

Peng & Parker (1997) recently presented a numerical procedure for solving an ideal jet impinging on an uneven wall, using a Hilbert transform and the generalized Schwarz–Christoffel transformation technique to obtain a system of nonlinear integro-differential equations. They present results for the impact of a jet of width 2 at normal incidence upon various walls. For example 7(a) $x(y) = e^{-y^2}$ (figure 7a, with the dotted lines representing the jet stagnation line), 7(b) $x(y) = -0.25e^{-(y-0.2)^2}$, and 7(c) $x(y) = -1.2 \operatorname{sech}(y - 0.85)$. As we used plots, their results do not compare exactly with ours but the drawing for a symmetrical wall is similar. When the barrier starts

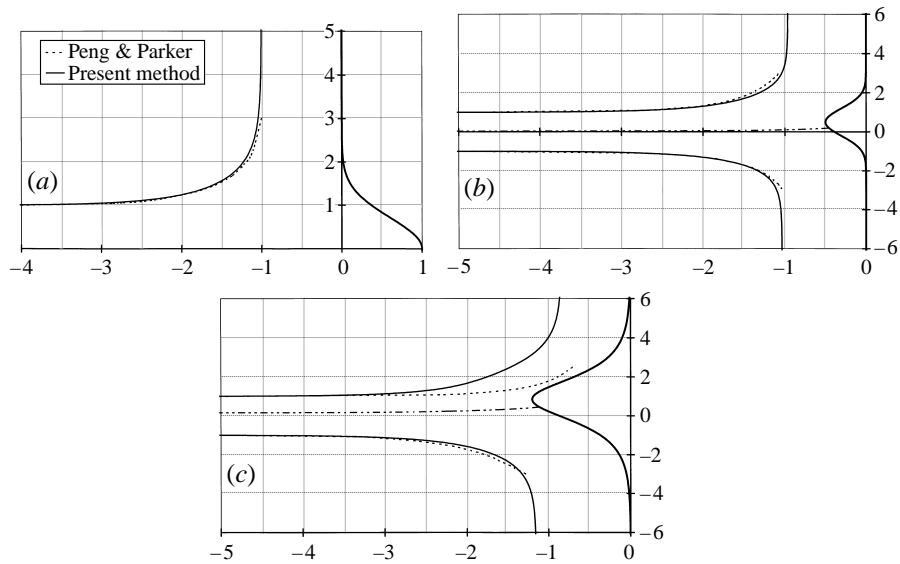


FIGURE 7. Impact of a jet of width 2 at normal incidence on symmetric and asymmetric walls: (a) $x(y) = e^{-y^2}$, (b) $x(y) = -0.25e^{-(y-0.2)^2}$, and (c) $x(y) = -1.2 \operatorname{sech}(y - 0.85)$.

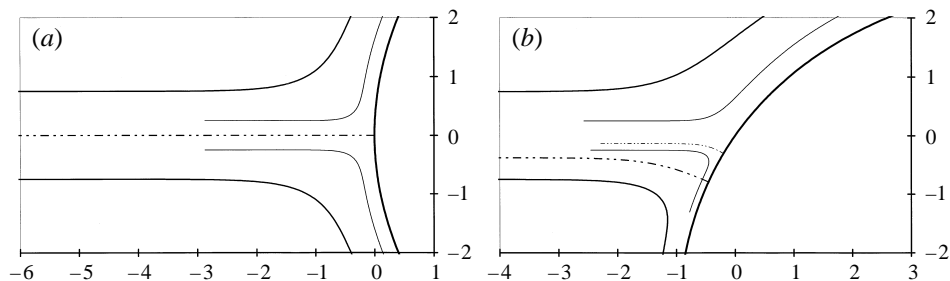


FIGURE 8. (a) Impact of a jet of width 0.5 and 1.5 at normal incidence on an arc of parabola extended by two plates. (b) The wall is rotated by an angle of 35° .

to become asymmetrical, the plots differ more and more. Conservation of mass does not seem to be verified in their plots, as the width of the incoming jet is greater than that of the sum of the two outgoing jets. So the asymmetric solutions would have to be revised, or at least other data would have to be used.

To test our method, we now consider other wall shapes close to the geometry of the streamlines we expect to find with impinging jets: an arc of parabola extended to infinity by two plates, with the origin O at the vertex of the parabola. Figure 8(a) shows the computations for symmetrical impact and for two given widths h_A (0.5 and 1.5). The wall is then rotated 35° (figure 8b). The pressure coefficient distribution $C_p = 1 - e^{2\tau}$ along these two barriers for $h_A = 1.5$ is presented in figure 9.

To show the possibilities of our method, we now consider a more complex wall shape consisting of two sinusoidal periods with wavelengths of 2, extended to infinity by two plates. The wall is inclined at an angle of 45° with respect to the direction of the centreline of the impinging jet. The jet width is 0.5 and the free streamlines that we calculated are plotted in figure 10.

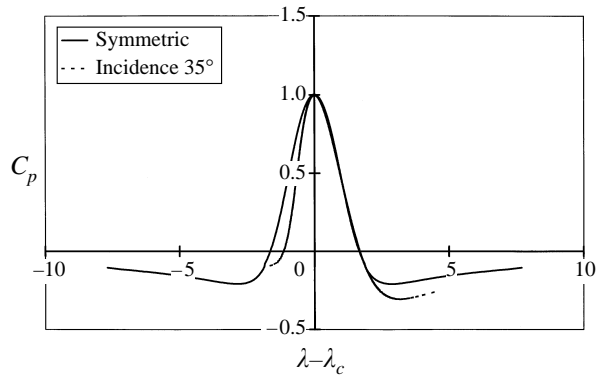


FIGURE 9. Pressure coefficient distribution along the two barriers for $h_A = 1.5$.

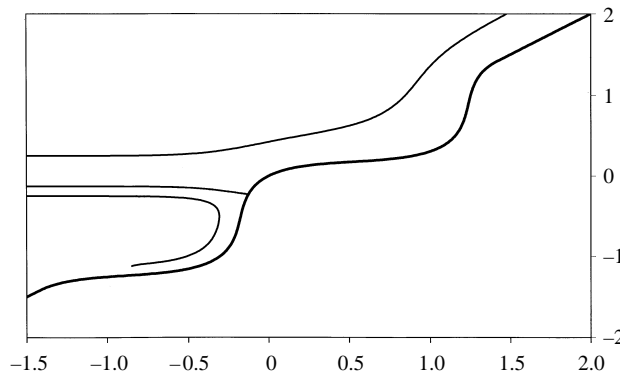


FIGURE 10. Impact of a jet of width 0.5 on a wall. The shape is given by two sinusoidal periods with wavelengths of 2 extended by two plates and is inclined at an angle of 45° .

3.3.2. Inverse problem

To our knowledge, there are no data for this problem in the literature so we will test our method by drawing the walls of the analytical and computed solutions that we studied above.

For symmetrical distributions, any symmetrical seed function ϵ_0 can be chosen. Using the analytical velocity distribution (or $\tau(s)$) of symmetrical barriers (jet impinging normally on a wall, or infinite wedge) in our other program, we can draw a wall that coincides exactly with the initial one. The velocity distribution from the symmetrical parabola (see figure 9) is then used to test the method. Here again, with any symmetrical function ϵ_0 , the designed wall is identical to the initial one (figure 11a). Convergence is reached after 20 iterations, requiring about one minute of calculation on a PC Pentium 120 MHz computer.

For asymmetrical barriers, the value of γ is not defined. So we can only verify that, when the solution of the direct problem is used as the function ϵ_0 , the wall corresponds. The process converges immediately, of course, and gives the right result. In the cases of a jet impinging on an inclined wall or an inclined parabola, the drawing is exactly identical to the initial barrier (figure 11b)).

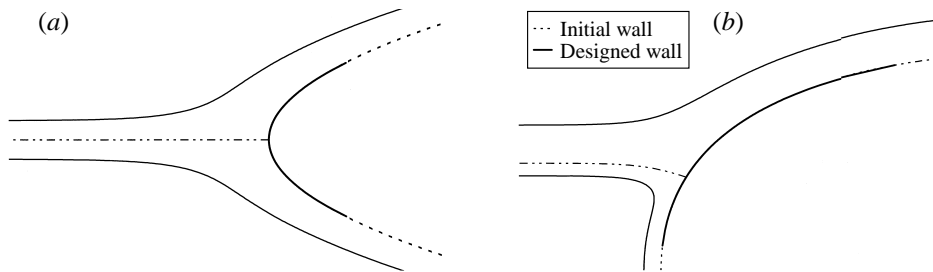


FIGURE 11. Inverse problem results.

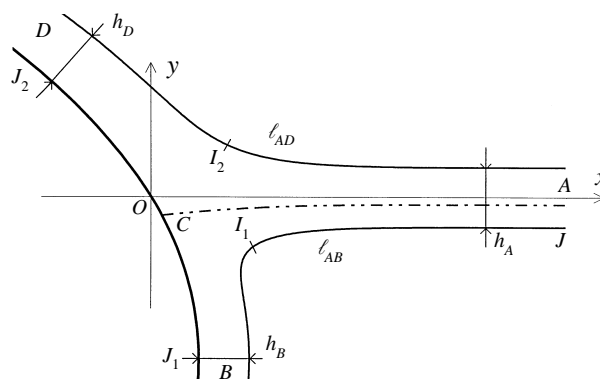


FIGURE 12. The inverse problem configuration for impinging free jets problem.

4. Impinging jets

The data of the problem are the widths h_1 and h_3 and the angles θ_1 and θ_3 (figure 1). The jets have the same speed V_∞ at infinity. The case of two impinging jets, requiring the streamline ℓ to be in equilibrium, is solved by coupling the direct and inverse problems. By rotating the flow pattern, the impinging jet J_3 can always be considered horizontal ($\theta_3 = \pi$).

To use the study of jet impact on a wall, we have to rotate the wall ℓ by an angle θ_1 . For the inverse problem, it is quite different. Now, the jet comes from the right of the barrier ℓ and not from the left as it did before (figure 12). In this configuration, the different mapping planes are changed (the points B and D are inverted), so few equations are modified. Equations (3.13) and (3.4) become

$$\tilde{\theta}(\sigma) = \frac{2}{\pi} \lim_{\zeta \rightarrow e^{i\sigma}} \operatorname{Re} \left\{ \int_0^\pi \frac{\zeta \sin \sigma'}{1 - 2\zeta \cos \sigma' + \zeta^2} \tilde{\tau}(\sigma') d\sigma' \right\} + \gamma + \frac{1}{2}\pi \quad (4.1)$$

because, in this case $\Theta(0) = \pi$, and

$$df = -\frac{V_\infty}{\pi} \left(\frac{h_B}{2 + \zeta + 1/\zeta} - \frac{h_D}{2 - \zeta - 1/\zeta} \right) \left(1 - \frac{1}{\zeta^2} \right) d\zeta \quad (4.2)$$

respectively.

From now on, we will index the values or functions relating to the direct problem by a superscript I, and those for the inverse problem with II.

4.1. Numerical procedure

The general problem can be stated initially with any arbitrary obstacle. We choose an infinite plane by considering the bisector of the two jet directions as a rigid barrier. The bisector must not be chosen for identical impinging jets ($h_1 = h_3$), because this is the solution to the problem. The origin of the arc lengths is first taken at the origin O of the Cartesian coordinates. Let the function $\theta_k^I(s)$, with $k = 1$, describe the initial wall; k is the iteration of the whole system (direct + inverse), which we will call the chief iteration.

The direct problem is first solved to calculate the speed distribution on this wall. This is done by solving the recursive scheme of the direct problem (index n for its iterations):

$$\begin{aligned} \epsilon_{k,n}^I &= (1 - r_1)f_1(\tilde{\tau}_{k,n-1}^I, \gamma_{k,n-1}^I, \lambda_{Ck,n-1}^I) + r_1\epsilon_{k,n-1}^I, \\ \tilde{\theta}_{k,n}^I &= (1 - r_2)f_2(\epsilon_{k,n}^I) + r_2\tilde{\theta}_{k,n-1}^I, \\ \tilde{\tau}_{k,n}^I &= (1 - r_3)f_3(\tilde{\theta}_{k,n}^I, \epsilon_{k,n}^I) + r_3\tilde{\tau}_{k,n-1}^I, \\ \gamma_{k,n}^I &= (1 - r_4)f_4(\tilde{\theta}_{k,n}^I, \epsilon_{k,n}^I) + r_4\gamma_{k,n-1}^I, \\ \lambda_{Ck,n}^I &= (1 - r_5)f_5(\tilde{\tau}_{k,n}^I, \gamma_{k,n}^I, \epsilon_{k,n}^I) + r_5\lambda_{Ck,n-1}^I. \end{aligned}$$

At convergence, this gives us the function $\tau_k^I(s)$ and the position γ_k^I of the dividing point, which will now be considered as the origin of arc lengths and of the Cartesian coordinates. The relative location of the impinging jet can be defined by drawing the stagnation streamline.

This velocity distribution $\tau_k^I(s)$ is used to initialize the inverse problem. γ_k^{II} will thus be equal to $\pi - \gamma_k^I$. The solution of the recursive scheme for the inverse problem, given

$$\begin{aligned} \tilde{\tau}_{k,n}^{II} &= (1 - r_1)f_1(\epsilon_{k,n-1}^{II}) + r_1\tilde{\tau}_{k,n-1}^{II}, \\ \epsilon_{k,n}^{II} &= (1 - r_2)f_2(\tilde{\tau}_{k,n-1}^{II}) + r_2\epsilon_{k,n-1}^{II}, \end{aligned}$$

can be used to define $\theta_k^{II}(s)$, which characterizes the new geometry of the wall.

Now, for the next iteration $k + 1$, we consider the impact of jet J_1 , not on the rotated wall but on the wall described by

$$\theta_{k+1}^I(s) = (1 - r)\theta_k^I(s) + r(\theta_k^{II}(s) - \theta_1).$$

The weighting factor r is chosen to belong to $[0.3, 0.5]$.

The process is reiterated until convergence, and is stopped by a test on the relative error associated with θ_k^I . About twenty chief iterations are necessary. The algorithm is presented in figure 13.

We should point out that we do not have to reach convergence with the direct problem at each chief iteration k . This is of no use because the wall geometry will always be wrong until convergence is reached, so the exact speed distribution is not needed. Moreover, solving for it is very time-consuming, so we perform just three iterations for the direct problem and 20 for the inverse one. All the results require about ten minutes of calculation on a PC Pentium 120 MHz computer.

4.2. Computed results

We have previously proposed taking $\theta_3 = \pi$. We should note here that we can also choose $h_1 = 1$ and $h_3 \leq 1$ by reversing jets J_1 and J_3 . This will be done from here on.

To test our method, we will compare our data with the few analytical results from the literature. They are: direct impact of jets of equal or different thickness, impact with incidence of two equal jets, and impact of shifted jets.

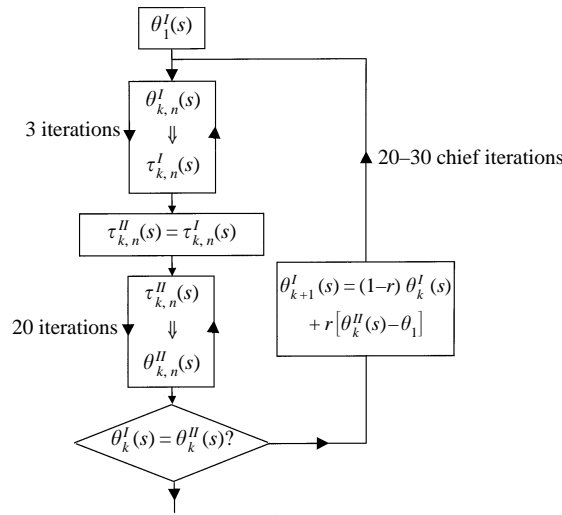


FIGURE 13. Algorithm of the method

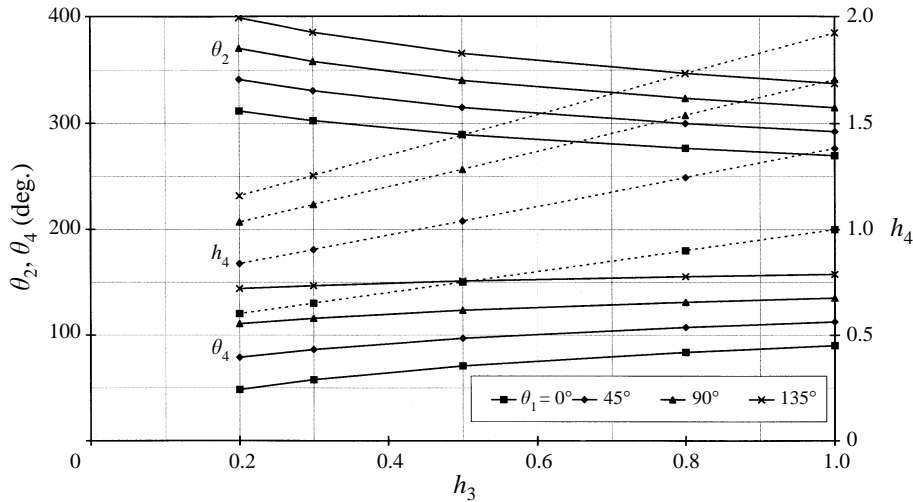


FIGURE 14. Variations of the angles θ_2 and θ_4 , and the thickness h_4 , versus h_3 for different angles of incidence θ_1 .

For general configurations (different jets at incidence), we could only verify the theorem of change of momentum, which is not used in our solution. With the notation defined in figure 1, this can be expressed

$$h_1 \cos \theta_1 - h_3 = h_2 \cos \theta_2 + h_4 \cos \theta_4, \tag{4.3}$$

$$h_1 \sin \theta_1 = h_2 \sin \theta_2 + h_4 \sin \theta_4. \tag{4.4}$$

Figure 14 shows the variations of the angles θ_2 and θ_4 , and the thickness $h_4 = 1 + h_3 - h_2$ versus h_3 for different angles of incidence θ_1 (0° , 45° , 90° , and 135°). This represents our computed results for all cases except shifted jets.

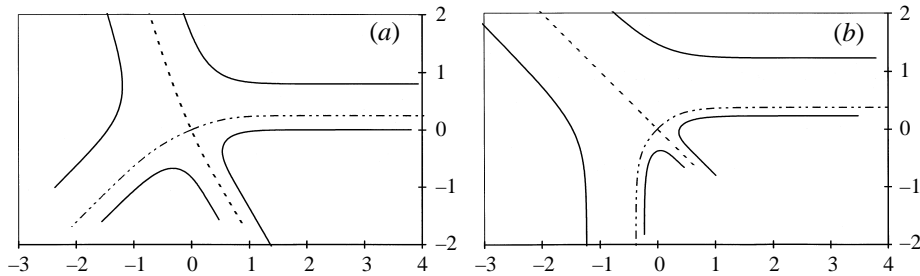


FIGURE 15. Impinging free jets. (a) $\theta_1 = 0^\circ$, $h_1 = 1$, and $h_3 = 0.5$, (b) $\theta_1 = 90^\circ$, and $h_1 = h_3 = 1$.

4.2.1. Analytical results

(i) Direct impact of two equal jets, $\theta_1 = 0^\circ$ and $h_3 = 1$

We have, directly

$$h_1 = h_2 = h_3 = h_4, \quad \theta_2 = \frac{3}{2}\pi, \quad \theta_4 = \frac{1}{2}\pi.$$

The plot of free streamlines we computed matches the analytical solution given by Milne-Thomson (1968):

$$y(x) = \frac{h_1}{2} + \frac{h_1}{\pi} \ln \left\{ \coth \left(\frac{2\pi x}{4h_1} - 1 \right) \right\}.$$

(ii) Direct impact of jets of different thicknesses (figure 15a), $\theta_1 = 0^\circ$ The conservation of mass and the theorem of change of momentum yield

$$h_2 = h_4 = \frac{h_1 + h_3}{2}, \quad \cos \theta_4 = \frac{h_1 - h_3}{h_1 + h_3}, \quad \theta_2 = 2\pi - \theta_4.$$

The computing method yields the analytical relations between h_2 and h_4 , and between θ_2 and θ_4 exactly. So (4.4) is obviously verified, which is not the case for (4.3). There is some difference between the computed value of θ_4 and the analytical: about 0.05° , or less than 0.1% in relative error. So, equation (4.3) is not strictly verified, and the relative error is defined

$$x_{rel}(\%) = \left| \frac{(h_1 \cos \theta_1 - h_3) - (h_2 \cos \theta_2 + h_4 \cos \theta_4)_{computed}}{(h_1 \cos \theta_1 - h_3)} \right| \times 100.$$

For $h_3 = 0.8$ and 0.5 , we get a relative error of about 0.2%. But in these cases, the half-unit circle of the ζ -plane is discretized the same way as for the impact of J_1 and J_3 , with 721 evenly distributed points. For better results, an irregular subdivision (981 points) can be used with many more quadrature points in the vicinity of 0 and π . So for $h_3 = 0.5$ the error is reduced to 0.02%. For $h_3 = 0.3$ or 0.2 , this irregular subdivision is used. In the case of $h_3 = 0.2$, the relatively unfavourable result for x_{rel} ($x_{rel} = 0.16\%$, 0.06% for $h_3 = 0.3$) can be explained by the fact that, as the thickness of the jet J_3 is small, the arc lengths on ℓ calculated during the inverse problem will be small. The infinite points B and D cannot be reached exactly. This is the phenomenon of crowding.

(iii) Equal jets with incidence (figure 15b), $h_3 = 1$ The special case of jets impinging at incidence could be considered as an analytical one. Indeed, if two equal jets impinge at incidence ($\theta_1 = 2\alpha$), it is clear that the solution will be symmetrical with respect to the bisector of the angles between the directions J_1 and J_3 . Furthermore, applying the principle of reversibility, the solution will be the same as in the previous case (direct

$y_1 - \tilde{y}_3$	$\theta_2(\text{deg.})$	$\frac{\Delta\theta_2}{\theta_2}(\%)$	$\theta_4(\text{deg.})$	$\frac{\Delta\theta_4}{\theta_4}(\%)$	x_{outlet}	y_{outlet}
0.7	280.541	0.02	100.652	0.07	0.003	-0.028
1.1	266.535	0.01	86.476	0.02	0.002	0.009
1.5	251.935	0.06	72.244	0.21	0.009	0.045

TABLE 1. $h_1 = h_3 = 1$

impact of different jets) if we reverse all the velocities. So we have

$$\begin{aligned} \theta_1 &= 2\alpha, \theta_2 = 3\pi/2 + \alpha, & \theta_4 &= \frac{1}{2}\pi + \alpha, \\ h_2 &= h_1(1 - \cos \alpha), & h_4 &= h_1(1 + \cos \alpha). \end{aligned}$$

The computed results for h_2 , h_4 , θ_2 , and θ_4 are identical to the analytical ones for the different values of θ_1 , so the relative errors associated with the theorem of change of momentum are almost zero (about $10^{-5}\%$).

(iv) Shifted jets. The case of shifted jets is completely determined because the distance between the axes of the two jets is requested. This configuration was studied by Birkhoff & Zarantonello (1957), and especially by Gurevich (1966), who gave

$$y_1 - \tilde{y}_3 = h_1 - h_2 \cos \theta_2 - \frac{1}{\pi} \left(h_2 \sin \theta_2 \ln \left| \tan \frac{\theta_2}{2} \right| + h_4 \sin \theta_4 \ln \left| \tan \frac{\theta_4}{2} \right| \right),$$

where $y_1 - \tilde{y}_3$ is the distance between the upper free surface of jet J_1 at infinity and the lower surface of jet J_3 . Later, Keller (1990) takes up this equation again. The programme has to be modified so the distance between the axes of the jets can be set.

Table 1 gives θ_2 , θ_4 , and their relative error in association with the analytical solutions, and the right-hand terms of the theorem of change of momentum x_{outlet} (4.3) and y_{outlet} (4.4). We present only results for $h_1 = h_3$, so the left-hand terms of equations (4.3) and (4.4) are equal to zero.

Our computed results seem to agree very well with the analytical solutions. So we will now treat jets of different thicknesses impinging at incidence, for which no data are available in the literature.

4.2.2. Other results

To emphasize the performance of our method, we will consider different values for the parameters θ_1 (45° , 90° , and 135°) and h_3 (0.8, 0.5, 0.3, and 0.2). In each case, the relation given by Keller for the distance of the asymptote from the stagnation point is verified (less than 0.05% on the relative error associated with y_L). As was previously done with equation (4.3), the relative error for (4.4) can be defined by

$$x_{rel}(\%) = \left| \frac{h_1 \sin \theta_1 - (h_2 \sin \theta_2 + h_4 \sin \theta_4)_{computed}}{h_1 \sin \theta_1} \right| \times 100.$$

An evenly distributed discretization was used for $h_3 = 0.5$ and 0.8, and an irregular subdivision for the other values. Usually, the errors x_{rel} and y_{rel} are low (about 0.05%) and can, if necessary, be reduced by fine discretization. We noticed some special cases – $\theta_1 = 45^\circ$ and $h_3 = 0.8$ or 0.5; $h_3 = 0.2$ and $\theta_1 = 45^\circ$ or 90° , – where $x_{rel} \simeq 0.5\%$. In the first case, it would be reasonable to think that the results would be better with a finer discretization on the half-unit circle. But these will probably not be as good as the others, because the left-hand term in equation (4.3) is very small (≤ 0.1). And as

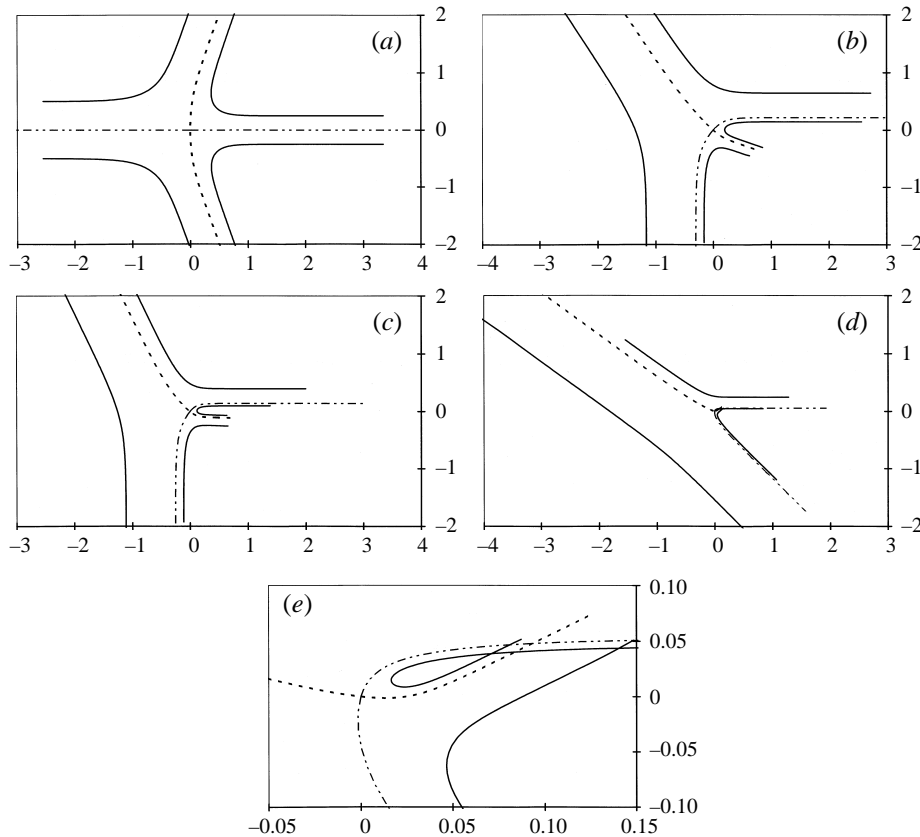


FIGURE 16. Impinging free jets. (a) $\theta_1 = 45^\circ$, $h_1 = 1$, and $h_3 = 0.8$, (b) $\theta_1 = 90^\circ$, $h_1 = 1$, and $h_3 = 0.5$, (c) $\theta_1 = 90^\circ$, $h_1 = 1$, and $h_3 = 0.3$, (d) $\theta_1 = 135^\circ$, $h_1 = 1$, and $h_3 = 0.2$, and (e) $\theta_1 = 135^\circ$, $h_1 = 1$, and $h_3 = 0.2$ – enlargement.

the absolute error is nearly the same in each configuration (10^{-4}), the relative error will always be larger. In the case of $h_3 = 0.2$, as pointed out previously, the points B and D at infinity are not reached exactly, even with fine discretization, and that is why the theorem of change of momentum is not verified exactly.

Figure 16 shows the computed jets for (a) $\theta_1 = 45^\circ$ and $h_3 = 0.8$, (b) $\theta_1 = 90^\circ$ and $h_3 = 0.5$, (c) $\theta_1 = 90^\circ$ and $h_3 = 0.3$, and (d) $\theta_1 = 135^\circ$ and $h_3 = 0.2$. An enlargement of the impinging area for the last case is plotted in figure 16(e). Like Dias *et al.* (1987) for jets exiting from nozzles, or Elcrat & Trefethen (1986) for flows over polygonal obstacles, the flow crosses itself, and hence is non-physical. This example is given to show that nothing in this formulation prevents this from happening. To determine the flow for this extreme configuration more realistically the mathematical model would have to be revised.

5. Concluding remarks

On the basis of these tests, we think that our method provides a reliable way of solving numerically the two-dimensional free-surface problem of two impinging free jets. The only limitation is the usual crowding. This is mainly true for large h_1/h_3 ratios and large angles of incidence, where we need many points in the vicinity of B

and D . We are quickly limited by the computed precision and, even then, the wall arc lengths are not long enough.

This solution shows that no additional assumptions are needed in order for the problem to be determined when it is considered as a boundary problem. This confirms that the problem is completely determined by the widths h_1 and h_3 of the incoming jets, and by the angle formed between them, contrary to all that has been published in the literature. Prescribing the streamline ℓ in equilibrium appears to be much more efficient than applying the theorem of change of momentum.

The inverse method we used, which is needed in order to deal with the problem of impinging jets, cannot solve an arbitrary inverse problem exactly, i.e. design the wall corresponding to a prescribed speed distribution. We are looking for a new formulation to solve this problem without specifying the value of γ . We will then have to check if any additional constraints beyond the speed distribution prescribed by Ω_S in the vicinity of the stagnation point need to be satisfied, as in airfoil design.

REFERENCES

- BIRKHOFF, G. & ZARANTONELLO, E. H. 1957 *Jets, Wakes and Cavities*. Academic Press.
- DIAS, F., ELCRAT, A. R. & TREFETHEN, L. N. 1987 Ideal jet flow in two dimensions. *J. Fluid Mech.* **185**, 275–288.
- DIAS, F. & VANDEN-BROECK, J.-M. 1990 Flows emerging from a nozzle and falling under gravity. *J. Fluid Mech.* **213**, 465–477.
- ELCRAT, A. R. & TREFETHEN, L. N. 1986 Classical free-streamline flow over a polygonal obstacle. *J. Comput. Appl. Math.* **14**, 251–265.
- GUREVICH, M. I. 1966 *Theory of Jets in an Ideal Fluid*. Pergamon Press.
- HUREAU, J., BRUNON, E. & LEGALLAIS, PH. 1996 Ideal free streamline flow over a curved obstacle. *J. Comput. Appl. Math.* **72**, 193–214.
- HUREAU, J. & LEGALLAIS, PH. 1996 Résolution du problème inverse pour un profil. *AAAF J.* **32**, 3.3–3.10.
- HUREAU, J., MUDRY, M. & NIETO, J.-L. 1987 Une méthode générale de numérisation d'écoulements avec sillage de Helmholtz. *C. R. Acad. Sci. Paris II* **305**, 381–334.
- JACOB, C. 1959 *Introduction Mathématique à la Mécanique des Fluides*, Gauthier-Villars.
- KELLER, J. B. 1990 On unsymmetrically impinging jets. *J. Fluid Mech.* **211**, 653–655.
- KING, A. C. & BLOOR, M. I. G. 1990 Free streamline flow over curved topography. *Q. Appl. Maths* **48**, 281–293.
- LEVI-CIVITA, T. 1907 *Scie e leggi di resistenza*, Rendiconti del circolo Mathematico di Palermo **23**.
- MILNE-THOMSON, L. M. 1968 *Theoretical Hydrodynamics* (5th edn). Macmillan.
- PENG, W. & PARKER, D. F. 1997 An ideal fluid jet impinging on an uneven wall. *J. Fluid Mech.* **333**, 231–255.